Prepared for submission to SPSC

NA64 Status Report 2024

The NA64 Collaboration[1]

CERN-SPSC-2024-024 / SPSC-SR-352
25/08/2024

[1] http://na64.web.cern.ch/

Abstract:

In this report, we focus mostly on the results obtained after unblinding the 2022 data using 160 GeV muons at the M2 beamline. We also report on the preliminary analysis of the 2023 data. Compared to 2022 an order of magnitude more statistics (1.5×10^{11} MOT) was collected with an upgraded setup featuring an additional magnetic spectrometer. The data show that the main background source from the miss-reconstruction of the incoming momentum is reduced by at least two orders of magnitude. Finally, we present the status of the ongoing 2024 run at M2 and give an overview of our plans before LS3 including the scenario of a possible run in 2026.

Moreover, we summarise the current status of the analysis for the 2023 data collected at H4 with a setup upgraded with a prototype of a veto hadronic calorimeter (VHCAL) to suppress the dominant background from large-angle hadronic secondaries produced in the primary beam interactions upstream of the active target. With the collected statistics of 4.4×10^{11} electrons on target (EOT), we demonstrate the effectiveness of this approach by reducing background to the negligible level and significantly improve the signal efficiency by increasing the missing energy threshold from 50 GeV to 60 GeV. The obtained results demonstrate the great potential of our approach and provide clear guidance for designing a full-scale optimized VHCAL (to be constructed during LS3) to make experiment background-free at a level of 10^{13} EOT that we expect to gather during RUN 4. This will allow us to enhance and extend the sensitivity for dark sector physics from future searches and decisively explore the well-motivated region of parameter space suggested by benchmark Light Dark Matter (LDM) models.

Our projections also show a significant gain when exploring LDM with the H4 e^+ beam via the annihilation channel since the mass range is extended. We also report on the run carried out at H4 in 2024. Preliminary results of a new LYSO-based synchrotron radiation detector prototype are presented together with the test of new faster electronics to readout the NA64 calorimeters. We conclude with our plans before LS3 including the scenario of a possible run at H4 in 2026.

Contents

1 Introduction

NA64 pioneered the active dump/missing energy technique in the quest for Dark Sectors. Using this approach, the current NA64 research program address the three most interesting and important complementary issues in dark sector physics that are accessible for thorough investigation at the CERN SPS:

(i) search for light dark matter and other BSM physics with masses below the electroweak scale ($\ll 100$ GeV) with the H4 electron/positron beams;

(ii) search for dark sector predominantly coupled to the second lepton generation which could provide solution to the muon g-2 anomaly and dark matter relic abundance with the M2 muon beam;

(iii) search for leptophobic dark sector predominantly coupled to light SM quarks with the SPS hadronic beams.

Recently, from the measurements at the H4 beamline, NA64 set the most stringent upper limits in the kinetic mixing (ϵ) and Dark Photon (A') mass plane for masses below 350 MeV. The collected data also allow to constrain the values of scalar and Majorana DM with coupling $\alpha_D \leq 0.1$ and $m_{A'} > 3m_\chi$ in the mass range $0.001 \leq m_\chi \leq 0.1$ GeV. The latest results with the 2016-2022 collected statistics were published in Phys. Rev. Lett. [1] and the paper was highlighted as an Editor's suggestion.

In this report, we present the first results for a search of Dark Sectors using 160 GeV muons from the M2 beamline. The publication was featured in the Physics Magazine of the American Physical Society (APS).

We also give an update on the status of the ongoing analysis of the data collected at M2 in 2023. In addition, we report on the preliminary results of the 2023 analysis of the H4 data using 4.4×10^{11} EOT. Finally, we summarise the outcome of our run at H4 during last spring and our future prospects.

2 NA64 at M2 beamline

2.1 Summary of the first results using a 160 GeV muon beam

Compared to our previous report, the data analysis was unblinded and the results were published. For the collected 1.98×10^{10}MOT, the expected background within the signal box is estimated to be 0.07 ± 0.03. The main background source comes from the momentum mis-reconstruction in the magnet spectrometer downstream of the target. After unblinding, we found no events compatible with an invisible Z' charged under $U(1)_{L_\mu - L_\tau}$ decay in the signal region. These results allow us to obtain the 90% confidence level upper bounds on the coupling as a function of the Z' mass

following the frequentist approach. In Fig. 1 our constraints for two scenarios are illustrated. The left plot considers the minimal or *vanilla* model where Z' decays only to neutrinos. The green band shows the $\Delta a_\mu \pm 2\sigma$ region for the Z' contribution to the $(g-2)_\mu$ anomaly. In this case, NA64μ limits exclude masses $m_{Z'} \gtrsim 40$ MeV and coupling $g_{Z'} \gtrsim 6 \times 10^{-4}$. On the other hand, in extended scenarios, the Z' can decay to DM particles. NA64μ could probe a portion of the $(m_\chi,\ y)$ parameter space, with $y = (g_\chi g_{Z'})^2 (m_\chi/m_{Z'})^4$. For $m_{Z'} = 3m_\chi$, chosen to be away from the resonant enhancement $m_{Z'} \simeq 2m_\chi$, and $g_\chi = 5 \times 10^{-2}$ (to probe the DM freeze-out prediction and the muon g-2 anomaly), our results constrain the dimensionless parameter y to $y \lesssim 6 \times 10^{-12}$ for $m_\chi \lesssim 40$ MeV. These limits are the first ones obtained using a high-energy muon beam [2]. These results open a new path to explore DS physics in a complementary way to present and future experiments and demonstrate the robustness of our novel technique based on missing energy-momentum which is planned to be used by other experiments such LDMX and M3 [3, 4]. The results have been published in Phys. Rev. Lett. and have been featured in the Physics Magazine of the American Physical Society (APS) [2].

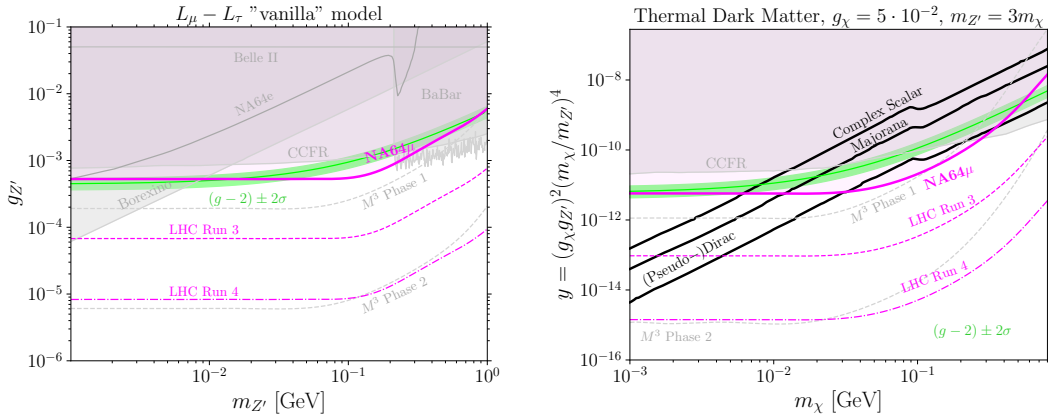

Figure 1. (*Left*) NA64μ 90% CL exclusion limits on the coupling $g_{Z'}$ as a function of the Z' mass, $m_{Z'}$, for the vanilla $L_\mu - L_\tau$ model. The $\pm 2\sigma$ band for the Z' contribution to the $(g-2)_\mu$ discrepancy is also shown. Existing constraints from BaBar [5, 6] and from neutrino experiments such as BOREXINO [7–9] and CCFR [10, 11] are plotted.(*Right*) The 90% CL exclusion limits obtained by the NA64μ experiment in the $(m_\chi,\ y)$ parameters space for thermal Dark Matter charged under $U(1)_{L_\mu - L_\tau}$ with $m_{Z'} = 3m_\chi$ and the coupling $g_\chi = 5 \times 10^{-2}$ for 1.98×10^{10} MOT. The branching ratio to invisible final states is assumed to be $\mathrm{Br}(Z' \to \text{invisible}) \simeq 1$. Existing bounds obtained through the CCFR experiment [10, 11] are shown for completeness. The thermal targets for the different scenarios are taken from [12](see [2] for more details). Existing constraints from other experiments, and projections before and after LS3 are also shown. See text for details.

Another publication summarising the details of our technique and our constraints to other scenarios as LDM in the context of Dark Photons, scalar mediators, etc. has

been completed and is currently under internal collaboration review. As an example, in Fig. 2, the 90% C.L. limits from NA64μ for scalar and vector (Dark Photon) mediators are illustrated. The plot on the left, shows the results for LDM searches using a muon beam. The current limit is not yet competitive compared to the other experiments but demonstrates our capability to probe masses above 100 MeV with higher statistics as shown with the projections for NA64μ before and after LS3. As shown in Fig. 2, combined with our electron and positron beam programs NA64 can probe the full parameter space of benchmark LDM models.

In the right plot of Fig. 2, the sensitivity in the case of a scalar mediator is depicted for the choice of parameters of coupling $g_\chi = 1$. Two different scenarios containing Dirac DM with the benchmark ratio $m_S/m_\chi = 3$ and the near-resonant regime $m_S/m_\chi = 2.1$ are considered. The corresponding thermal targets are extracted from [13]. Our limits cover part of the parameter space compatible with masses $m_S \leq 300$ MeV up to a coupling $g_S \sim 10^{-3}$ for the mass ratio $m_S/m_\chi = 3$. In the case, $m_S/m_\chi = 2.1$, the limits are only covering scalar masses up to $m_S \sim m_\mu$. More details on (i) the Monte Carlo (MC) approach used in simulating the signal events, (ii) systematics in the signal yields and (iii) level of background extracted from data can be found in [2]. For completeness, we show the projected sensitivities from the muon experimental program are shown both before the CERN Long Shutdown (LS3), or *LHC Run 3*, and after LS3, *LHC Run 4*. The computation of those limits is based on the foreseen detectors' upgrade to cope with higher beam intensities and (ii) the background reduction due to improvement of the experimental set-up configuration (see further details in the next section).

2.2 Preliminary results from the 2023 run

The results obtained from the 2022 analysis drove the optimisation of the 2023 muon run. We collected 1.5×10^{11} MOT with a significantly improved setup and an average intensity two times higher than in 2022, $5.6 \times 10^6 \mu$/spill. Here, we report the preliminary results of the ongoing analysis which gives already a very promising indication that the main background source, identified in the 2022 data set arising from mis-reconstruction of the muon momentum, is suppressed by more than an order of magnitude. The level of background is expected to be considerably reduced due to modifications of the experimental set-up sketched in Fig. 3. We summarise below the most relevant improvements:

- The major upgrade for the 2023 run is the addition of a third magnet spectrometer, MS1, upstream of the ECAL interaction point, effectively reducing the 80 meters long level-arm associated with the BMS region (BEND6 spectrometer) to ~ 6 meters.

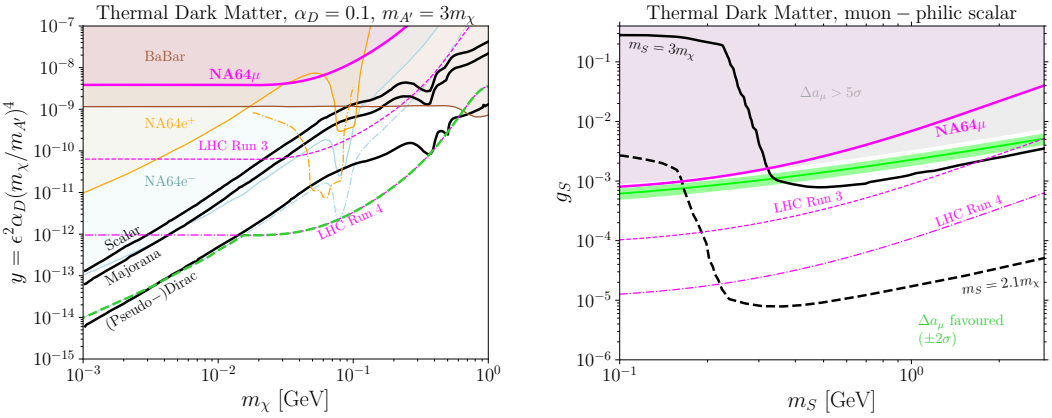

Figure 2. NA64μ 90% CL excluded limits with 1.98×10^{10} MOT and projected limits for the LHC Runs 3 and 5 for Light Dark Matter mediated by a Dark Photon (*left*) and for a muonphilic scalar mediator S (*right*). Existing constraints from other experiments, and projections using electron and positron beams are also shown (see text for details). In the scalar case, the thermal freeze-out target for Dirac DM is illustrated as computed in [13] for the scenarios with $g_\chi = 1$ and $m_S/m_\chi = 3$ (solid black line) and $m_S/m_\chi = 2.1$ (dashed black line). The "kink" around $\sim 2m_\mu$ is related to the opening of a new kinematically accessible channel, namely the DM annihilation to muons.

- To improve the momentum reconstruction and boost the efficiency we added 8 new trackers for a total of 23: 11 MMs (eight 8×8 cm^2 and three 25×8 cm^2), 4 GEMs, and eight straw stations (two 120×60 cm^2 and six 20×20 cm^2).

- The position of MS1 was chosen to further reduce the level of kaons in-flight decays with final-state muons, $K \to \mu + X$, given a shorter distance from the point of measurement of $p_{\rm in}$ to the target. The suppression factor is of the order $\sim 10^{-1}$. This background could be further reduced by proper identification of the kaons along the beam-line employing Cherenkov counters with achromatic ring focus (CEDAR).

- The addition of a second prototype VHCAL in the experimental set-up reduces the level of non-hermeticity of the detectors, due to a better rejection of events from upstream interactions with large-angle scattered secondaries.

- The trigger system was improved, including an additional scintillator counter, S_2 in the sketch, to have a better muon telescope and select the beam core. In addition, a veto counter, BK, was placed next to S_4 to remove the remaining part of the undeflected beam allowing us to reach intensities a factor of two higher than in 2022. The final trigger was $S_0 \times \bar{V}_0 \times S_1 \times S_2 \times S_4 \times \bar{BK} \times S_\mu$.

To measure accurately the level of momentum mis-reconstruction and the correlation between the momentum measured in the new MS1 spectrometer and in MS2

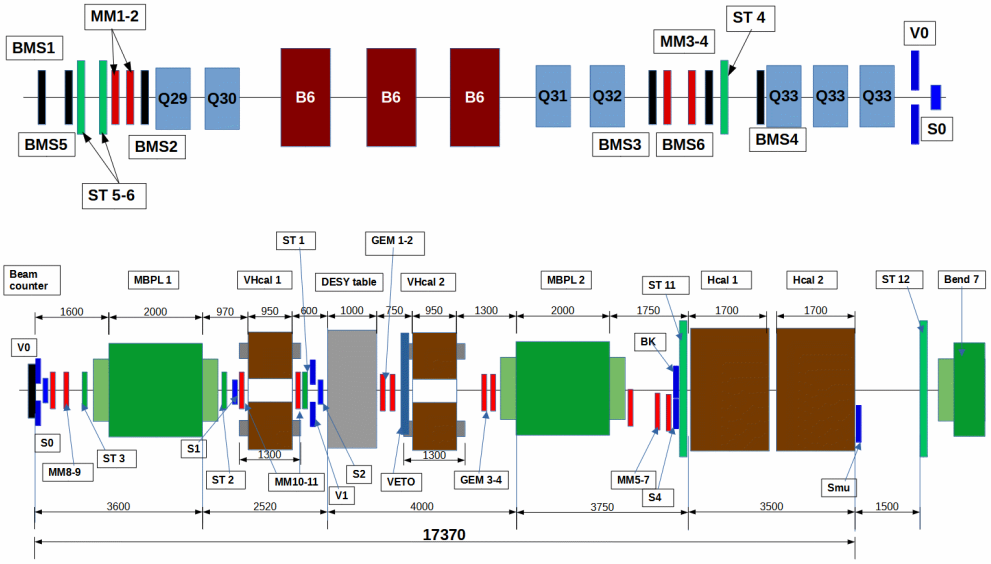

Figure 3. Sketch of the 2023 setup at M2.

we collected 1.3×10^{10} MOT without our target placed along the beam line with the physics trigger while 1.3×10^{6} MOT were collected with the calibration trigger $(S_0 \times \bar{V}_0 \times S_1 \times S_2)$). In this document, we report on the preliminary results achieved using a 10% of that data sample corresponding to about 1.3×10^{9} MOT. We apply the following selection criteria:

- *a single muon traversing the set-up*: there is only one single track in the upstream and downstream spectrometers (MS1 and MS2).
- *initial muon momentum at 160 GeV*: there is one single track selected in the momentum window [140, 180] GeV reconstructed in MS1.
- *Single hit in the detectors and clean track after MS2*: the tracking detectors located after the MBPL magnet have at most one hit.
- *No energy deposit in the two VHCALs*: an energy below 1 GeV in each VHCAL calorimeter is required.
- *MIP-compatible energy deposit*: in each calorimeter, respectively ECAL and HCAL, the energy deposit is compatible with a MIP. Additionally, a MIP signal in the central cell of the Veto is required before VHCAL. An event is accepted if its energy is less than 1.5 of these values. This cut allows the removal of events

compatible with muon-nuclear interactions in the target when the ECAL is present.

In Fig. 4 the momentum reconstructed in the new MS1 spectrometer is shown versus the one reconstructed in MS2 at the first and later stages of the selection criteria. As it is visible in the plot we find a good correlation between the momentum upstream and downstream the setup. In addition, we can see that a selection in the purity of the 160 GeV momentum measured in MS1 reduces the tails of the distribution. The preliminary background level is obtained by fitting the tail of the distribution towards the upper limits of the signal box, $p^{\rm up}_{\rm MS2} = 80$ GeV/c, and is reduced by at least one order of magnitude with respect to the 2022 result. Although these results are preliminary, they are already very encouraging, indicating the key role of MS1 in the analysis improving the reconstruction of the initial muon momenta. For completeness, in the bottom plot of the figure we illustrate the hermeticity plots after the selection criteria. The bulk of events with momentum in MS1 around 160 GeV but with lower momentum in MS2 correspond also with events with high energy deposit in the hadronic calorimeters. Those events result from the possible muon-nuclear interactions suffered by the muon from MS1 to MS2.

A similar study was carried out with physics runs using calibration trigger with the ECAL inside the setup and a sample of 8×10^6 MOT (50 % of the total statistics collected in this configuration). The preliminary results after applying the selection criteria are illustrated in Fig.5. The improvements in the setup would allow us also to gain at least a factor 2 in efficiency with respect to 2022 analysis.

2.3 Progress on the ongoing 2024 run and future prospects

This year we were granted 50 days of beam time from July 17th until September 4th. The removal of all beam elements in our setup and transport of detectors from H4 beam line started on July, 17th. Thanks to the work carried out by the transport and BE-EA departments most of the equipment was installed on July, 22nd. The installation was completed on July 26th, when we got the safety clearance and we started the commissioning and calibration of the detectors. The setup for this run was similar to the one used in 2023. The main relevant change was the addition of more trackers in the MS1 spectrometer (instead of 6 we have 8 this year) and in MS2 spectrometer. This year we have 3 Micromegas, two 20×20 cm^2 and three 120×60 cm^2 straw chambers.

With the combined 2023-2024 statistics we will be able to fully probe the remaining parameter space for an explanation of the $(g-2)_\mu$ anomaly in terms of Z' (L_μ-L_τ) and part of the very interesting LDM suggested region. With the total statistics of $\sim 3 \times 10^{11}$ MOT, we will be sensitive to dark photons in the high mass region not accessible with our measurements at H4 in electron and positron modes, thus, evidencing the complementarity of these programs.

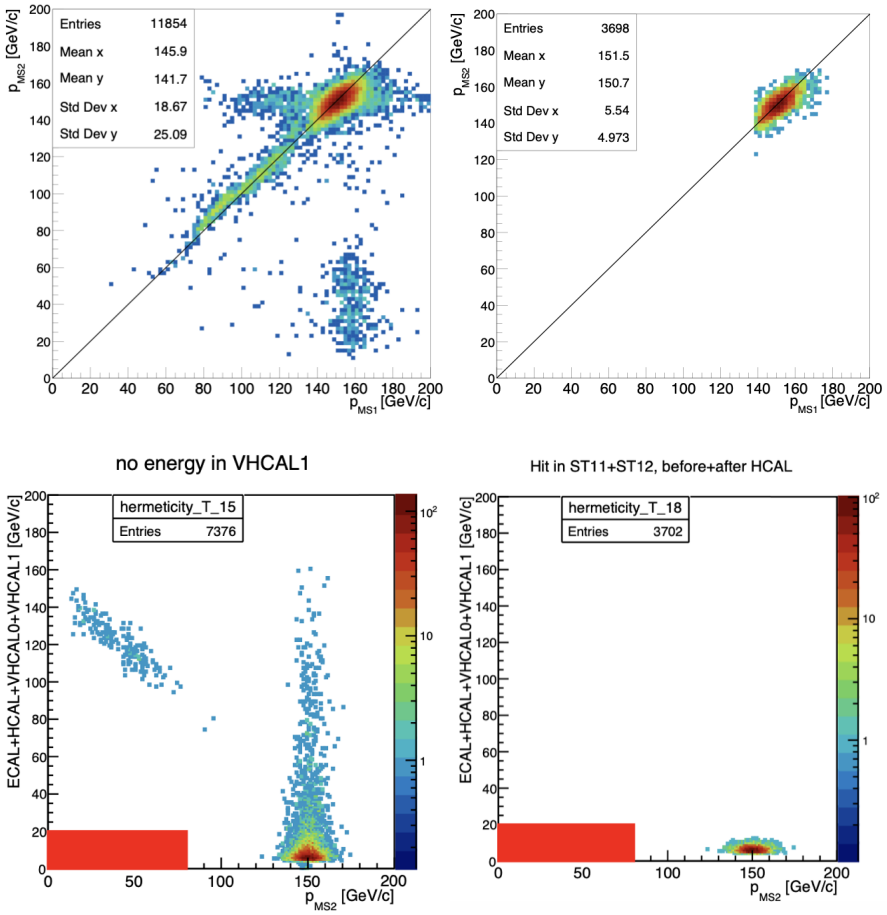

Figure 4. Preliminary results on 1.3×10^9 MOT collected using physics trigger and the ECAL moved out of the setup: *Top:* Momentum in MS2 versus Momentum in MS1 at the earliest and later stages of the selection criteria. *Bottom:* Sum of the collected energy in the calorimeters versus MS2 momentum.

For 2025 we do not plan to run at M2 as agreed with the other users. However, if LS3 would be postponed by one year we could consider running in 2026 to test some upgrades which could be prepared in 2025 such as a segmented trigger and a scheme for suppression of kaon background.

The ongoing analysis based on 2023-2024 data is essential to drive the optimization of the setup design and detector upgrades for the post-LS3 program of NA64 at M2 when two orders of magnitude larger statistics could be collected. This would enable the full exploitation of the physics potential of this program ensuring that CERN remains at the forefront of this research field.

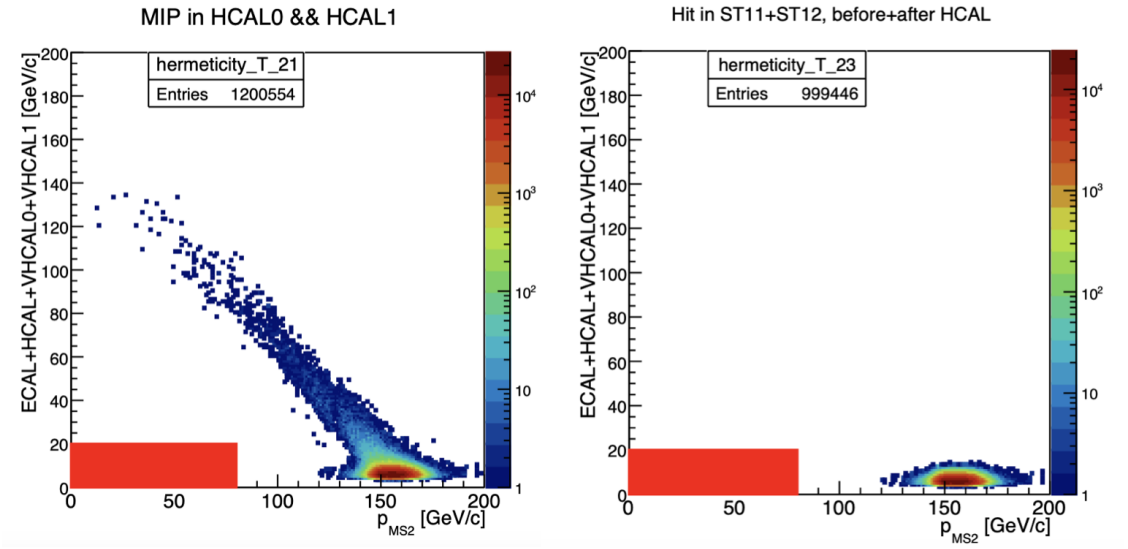

Figure 5. Cut-flow summary on the 8×10^6 MOT with calibration trigger at the last stages of the selection.

3 NA64 at H4 beamline

3.1 Outcome of the 2023 run and results from VHCAL prototype test

In 2023, we were granted by SPSC 55 days of beam time at H4 beamline, from the 10th of May until July 4th. The primary goal for this run was to improve our sensitivity to search for LDM produced through $A' \rightarrow$ invisible decays and test a VHCAL prototype that serves as an additional efficient veto against upstream electro-production of large-angle hadrons.

The setup, illustrated in Fig.6, is composed of a set of scintillators and veto counters (S_{0-3} and V_{1-2} in the sketch), a magnet spectrometer consisting of two dipole magnets (MBPL), and a set of tracking detectors which allow tagging the electron incoming beam. The tracking system, four Micromegas chambers (MMs), four straw detectors and two GEM detectors, allows a momentum measurement with a precision of $\delta p/p \sim 1\%$ [14]. A synchrotron radiation detector (SRD) [15] is used for electron identification allowing to suppress the hadron contamination in the beam ($\pi/e^- < 3\%$). The active target is a 40 radiation length (X0) high-efficiency shashlik electromagnetic calorimeter (ECAL) segmented in a matrix of 5×6 cells made of a sandwich of lead and scintillator plates.

The prototype veto hadronic calorimeter (VHCAL) made of Cu-Sc layers was placed after the SRD surrounded upstream and downstream by trackers. This calorimeter of size $500 \times 500 \times 1000\,\mathrm{mm}^3$ consists of 30 layers, each made of 25 mm copper and 2 mm of scintillating material. The VHCAL serves as an additional efficient veto against upstream electroproduction of large-angle hadronic secondaries.

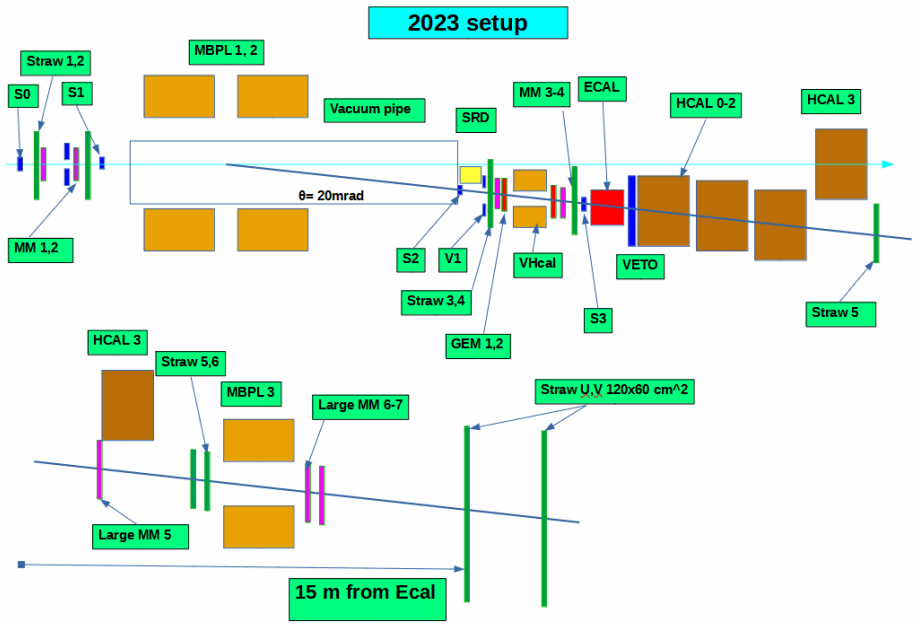

Figure 6. Schematic illustration of the NA64 setup used during 2023 run to search for the $A' \rightarrow$ invisible decay at H4.

The detector was tested in 2021 and 2022 NA64$_\mu$ pilot runs at M2, but we did not install it in 2022 to have a large sample of events in the same configuration as in 2021 to assess the background level with more statistics. After the analysis of the 2022 collected data [16] we decided to install the prototype during 2023 run to further reduce the background from neutrals secondaries escaping the HCAL acceptance. We optimised the setup to install the VHCAL without increasing the distance between the HCAL and the end of the vacuum window. In addition, we tried to minimise the amount of material along the line optimising the position of the scintillator counters and trackers after the MBPL magnets.

The setup is completed with a large high-efficiency VETO counter and three 7.5λ iron hadronic calorimeters (HCALs) to close the hermeticity of the setup measuring any energy leakage. One HCAL module is placed at the zero deflection line to veto charged and neutral secondaries produced from the electron interactions in front of the MBPL magnets.

A second magnet spectrometer was placed downstream of the last HCAL to measure processes involving muons in the final state after electron interactions in the target. In particular, we will be able to study processes involving $e^- \rightarrow \mu$ conversion [17]. The feasibility studies based on simulations to search for such a process have been recently summarised in [18]. Moreover, with this spectrometer, we will be able to characterise the energy distribution and the angle between the di-muons produced in the rare QED process. This is an important benchmark process and thus validating the MC is essential to have a reliable estimate of signal efficiency,

background and systematics.

3.1.1 Status of the 2023 analysis

We are in the process of finalizing the reconstruction and the blinded analysis of the statistics collected in 2023. Alongside the introduction of the VHCAL prototype, the data analysis for 2023 has benefited from several improvements. A pre-scaler was included in our trigger system to save calibration trigger events in parallel with the physics data. In this way, we can constantly monitor the variations in the response of every calorimeter cell throughout the data taking. This information is then included as spill-by-spill and run-by-run corrections to the energies of all calorimeters. Moreover, the track fitting procedure has been improved allowing us to set stricter constraints on the reconstructed momentum. This has further contributed to the suppression of the hadronic background from large-angle secondaries resulting from interactions upstream of the ECAL, while keeping a high efficiency for electron events.

The role of the VHCAL prototype in the analysis is highlighted in Fig. 7. Requiring an energy deposition below the expected noise in the VHCAL effectively removes the events in the region ($E_{\mathrm{ECAL}} < 70\,\mathrm{GeV}$; $E_{\mathrm{HCAL}} < 5\,\mathrm{GeV}$) for the selected period of runs. This topology of events corresponds to large-angle hadrons produced in the upstream beam material that miss any detection in the HCAL. Thanks to the hermeticity provided by the VHCAL prototype and stricter track selection criteria, the estimated contribution from large-angle hadrons from upstream electron-nuclear and photon-nuclear interactions appears to be reduced by at least one order of magnitude in the selected period. These numbers were evaluated from the extrapolation of events in the side-band ($E_{\mathrm{ECAL}} > 60\,\mathrm{GeV}$; $E_{\mathrm{HCAL}} < 1\,\mathrm{GeV}$) into the signal region.

The improvements in the analysis and monitoring allow us to have a better estimation of the remaining fraction of muons in the beam. Those muons can decay $\mu^- \to e^- + \nu_\mu + \bar{\nu_e}$ and mimic our potential signal candidates. This year, we have estimated the muon contamination in the beam and the probability of a muon being misidentified in the SRD as an electron by comparing the selection of events with muon-like signature in our detectors for both calibration and physics trigger events. This data-driven approach provides more accurate results than the ones obtained previously from simulations. The stability of the calorimeter response due to the constant monitoring is crucial for the identification of muons using HCAL and VETO detectors, in which MIP-compatible energy depositions are selected to extract μ-like events. Additionally, an improved suppression of pile-up events results in a reduced probability of beam muons passing the SRD selection due to a pile-up electron. Together, the muon contamination obtained is at approximately 2×10^{-5}. This results in a total expected background from muon decays at the level of 0.012 ± 0.006.

In order to gauge the extent of our improvements, the remaining events after the complete selection criteria of two periods are compared in Fig. 8 from 2022 and 2023

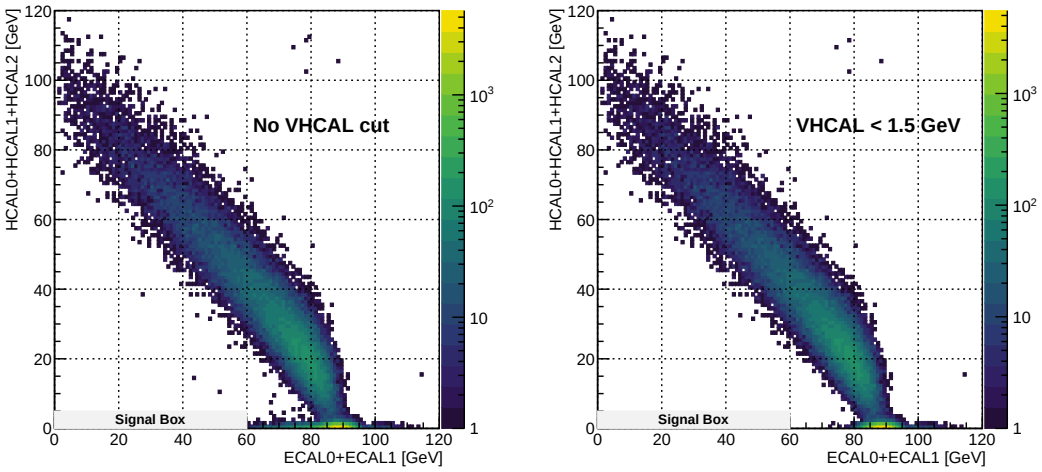

Figure 7. Distribution of events in the $(E_{\mathrm{ECAL}}; E_{\mathrm{ECAL}})$ plane before (left) and after (right) applying a cut on the total VHCAL energy for the same period shown in Fig. 8, after all other selection criteria are applied. Most of the events removed by the VHCAL cut lie close to the signal box and likely correspond to secondary hadrons that escape the HCAL acceptance.

analyses. The period selected for 2023 corresponds to roughly a third of the statistics accumulated in that year. The key difference is the cleaner separation between the signal region and the region populated by SM interactions. The preliminary results indicate that we can extend our signal region in the ECAL energy (E^{sb}_{ECAL}) from 50 GeV to 60 GeV as we expect to remain background-free.

This extension of the signal region increases our sensitivity to dark matter production via dark Bremsstrahlung and the effect is greater in the case of the resonant annihilation production channel. This is because the enhancement in the dark photon mass is restricted to the region $\sqrt{2m_e E^{sb}_{\mathrm{ECAL}}} \lesssim m_{A'} \lesssim \sqrt{2m_e E_0}$, where E_0 is the beam energy. The preliminary projections for the 90% C.L. exclusion limits expected from 2016-2023 statistics assuming zero background is depicted in Fig. 9. The comparison of these projections for the two signal region definitions is also visible in the figure.

In light of these results, the study and development of an optimized VHCAL detector for the electron mode setup has been started. Furthermore, these results validate our approach and technique, as we expect our statistics accumulated until LS3 to remain background-free.

3.2 Summary of the 2024 run

In 2024, the SPSC granted us 8 weeks of data taking from the 24th of April until the 19th of June. We used the same setup as in the 2023 run. The commissioning and calibration of the detectors, the beam and trigger tuning lasted approximately 10

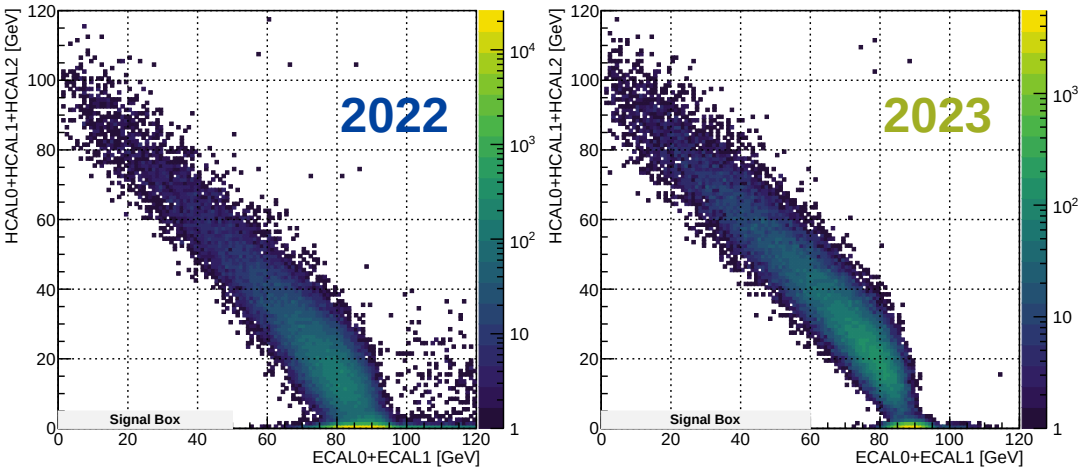

Figure 8. Comparison of the distribution of events in the $(E_{\mathrm{ECAL}}; E_{\mathrm{ECAL}})$ plane obtained for periods of runs in 2022 (left) and 2023 (right) after all selection criteria are applied. The periods selected for these plots correspond to a similar number of EOT: 1.66×10^{11} EOT and 1.49×10^{11} EOT, for 2022 and 2023, respectively. The signal box displayed is extended along the vertical axis to 5 GeV for illustration purposes.

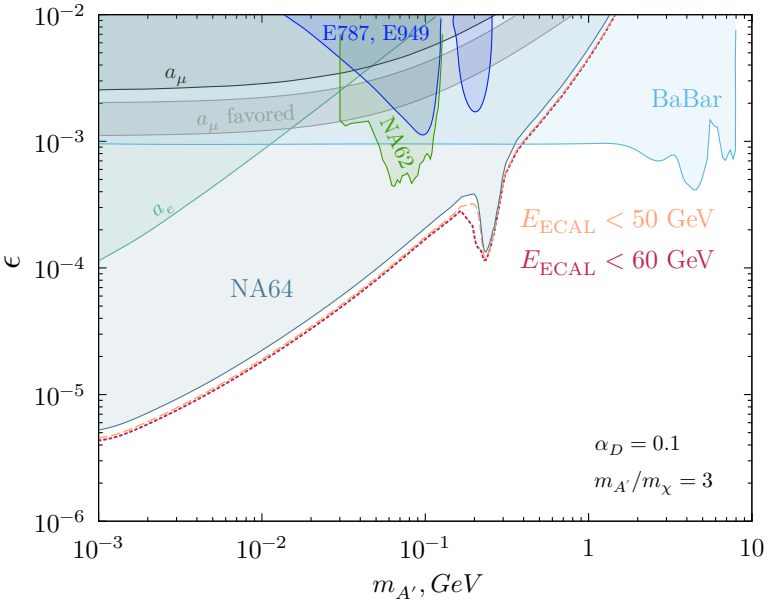

Figure 9. Preliminary NA64 90% C.L. exclusion limits (dashed lines) obtained for the $A' \rightarrow$ invisible search in the $(m_{A'}, \epsilon)$ plane for the combined 2016-2023 statistics. We compare the limits for two choices of the missing energy threshold in the ECAL: $E_{\mathrm{ECAL}} < 50$ GeV in **orange** and $E_{\mathrm{ECAL}} < 60$ GeV in **red**. This is only applied to the 2023 dataset and showcases the improved sensitivity enabled by the recent upgrades.

days. These days were also dedicated to testing the future upgrades of the calorimeter electronics and the new SRD detector foreseen after LS3. A detailed description of

the outcome of the tests will be given in the next section.

We started data taking the 7th of May at an average intensity of 6.5×10^6 e^-/spill. Similarly to 2023, we had excellent beam quality with most of the time 100 units on average on T2 target and many periods with 3 spills per cycle. Further tuning of the beam and the addition of extra vacuum (performed together with N. Charitonidis and S. Girod) allowed us to further reduce the beam halo to 3% and the hadron contamination 0.4% even at higher intensities. We collected 5.2×10^{11} EOT in 37 days. A summary of the spills accumulated along our run is shown in Fig. 10.

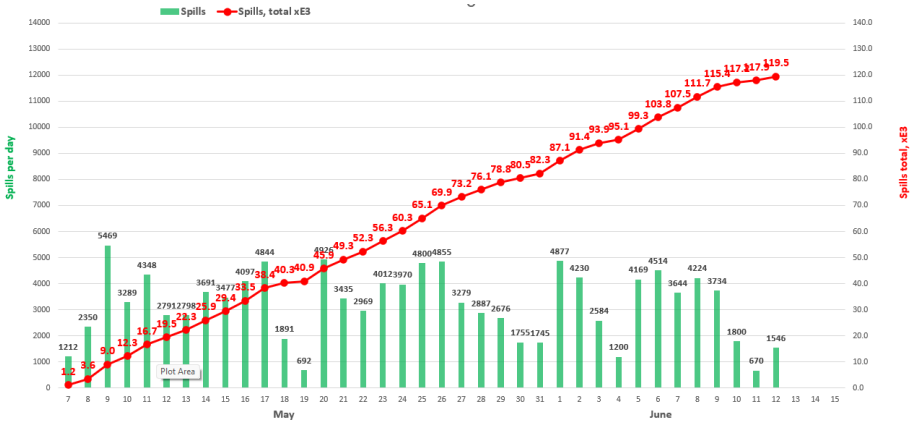

Figure 10. Spills recorded per day during the 2024 run at H4.

This year we tested also together with N. Charitonidis the maximum intensity delivered by the line and the maximum intensity at which the quality of the beam fulfills our requirements in terms of halo. We collected a few runs at intensities up to 13×10^6 e^-/spill. From the preliminary analysis, we verified that with an increase in intensity up to 9.4×10^6 e^-/spill we get a similar halo rate as at 6.5×10^6 e^-/spill.

After the long technical stop, from 12th to 15th of June, we switched to positrons at 70 GeV to increase the statistics collected in 2023. In addition, the new LYSO-based SRD detector was tested. Due to a problem with the accelerator and the needed exchange of a magnet, we lost additionally two more days. The total statistics collected was 2.25×10^{10} positrons on target.

3.2.1 Outcome of new front-end electronics test

In previous years, dedicated measurements were performed to demonstrate the improved performances of the electromagnetic calorimeter when using the new "Waveboard" (WB) digitizer from INFN to read signals from PMTs, in particular in terms of pile-up reduction and ECAL resolution improvement. The obtained results motivated us to further proceed in this direction, working on the development of a new dedicated firmware to integrate the device in the main NA64 DAQ and on the commissioning of the boards within the NA64 experiment data taking.

In Winter 2024, the integration activity was completed at INFN-Genova. Specifically, a new firmware for the "Waveboard" was implemented allowing the integration of the latter within the NA64 DAQ system employing the custom UCF (Unified Communication Framework) protocol, already used in NA64 to acquire data from the TDCs reading signals from Straw chambers. This activity involved the development of different IP cores, including the hardware-specific ones associated with the GTX fast MGT transceivers connected to the board of the laser driver. A key aspect of the firmware development is the generation of the WB internal clocks, to ensure proper synchronization with the other readout boards. To do so, the recovered 155.52 MHz clock from UCF link, synchronous with the main experiment clock from TCS, was used as the main reference for the on-board SI5345 PLL, which in turn generates the 233.38 MHz clocks for the ADCs. The FPGA MGT transceiver was configured to operate in a non-standard mode[1] to avoid the ambiguity associated with the clock recovery operation from the fast serial data from the MGT transceiver, that would otherwise translate to an acceptable clock jitter up to 6.4 ns. Finally, synchronization with the main TCS clock, operating at 38.88 MHz, was achieved by syncing the phase of the 155.52 MHz clock from PLL with the trigger signal extracted from the UCF data flow, which, by design, is phase-synchronous with the main TCS clock. Another important firmware feature that was introduced is the possibility to operate each channel in "zero-suppression mode", to reduce the overall data flow. In this mode, for each trigger, samples recorded within the readout window are transferred via UCF to the DAQ system only if the difference between the pedestal and the signal peak is larger than a programmable threshold. In parallel with the firmware development, all the software components to configure and monitor the board parameters were implemented, such as the readout window latency and size, or the rate of incoming triggers. To do so, the EPICS [19] framework and common tools were exploited, developing the necessary software components running on the ARM CPU hosted on the Waveboard. The development of all software components necessary to read data from WB in the NA64 reconstruction framework, `p348-reco`, used both for online data monitoring and for offline reconstruction and analysis, was completed.

During NA64 run at H4 in 2024 and after a full characterization of each WB at INFN-Genova, a full integration and commissioning test of the boards was performed, connecting the output signals from the PMTs coupled to the 60 ECAL cells to five WB devices (see also Fig. 11, left panel). A snapshot of the acquired raw data for events with a 100 GeV e^- hitting the central cell is reported in the right panel of the same figure. The observed $\simeq$ 25 ns time jitter is due to the intrinsic design of the TCS system trigger generator, operating at 38.88 MHz; in the offline analysis, this is compensated by subtracting, event-by-event, the trigger time measured in the same clock domain (the so-called "master time").

[1] This is the so-called "PMA" mode for the transceiver `RXSLIDE` module.

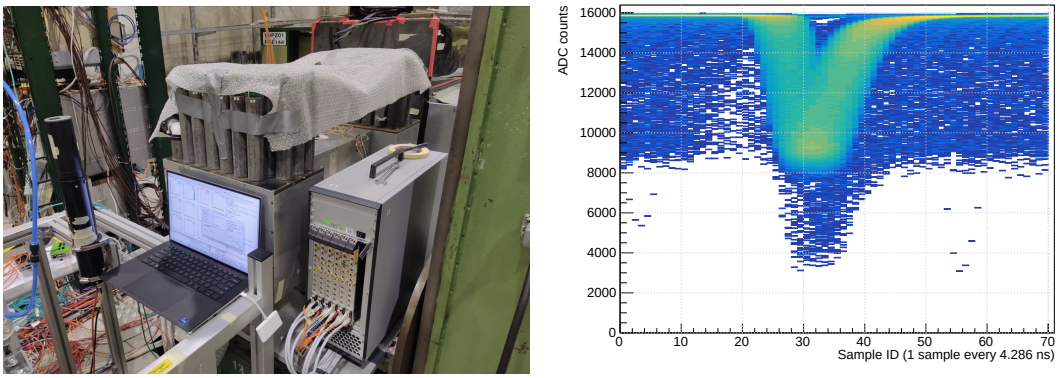

Figure 11. Left: the five Waveboards used to acquire signals from the NA64 ECAL PMTs, hosted in a mini-VME crate on the DESY platform close to the detector. Right: ECAL central cell online waveform data for events with a 100 GeV e^- hitting the ECAL center. The observed $\simeq$ 25 ns signal jitter is entirely due to the TCS trigger generator and is compensated in the offline analysis by compensating, event-by-event, for the measured trigger time.

First, the ECAL cells were individually calibrated. Later, different data-taking runs were collected, with the beam impinging on the central ECAL cell, for different intensities reaching up to 1.4×10^7 particles/spill. The trigger for the DAQ system was provided by the coincidence of the beam-defining plastic scintillator counters, with a corresponding rate of about a few kHz after prescaling.

For all intensities, no issues were observed with the boards, and data quality was confirmed by the online monitoring system. As an example, Fig. 12 shows the ECAL energy distribution for 100 GeV e^- events collected with beam intensity $\simeq 1.2 \times 10^7$ (blue curve), after applying preliminary calibration constants to all cells. For comparison, the result obtained from a calibration run collected in the 2023 session, with data acquired with MSADC devices and processed through the full analysis chain, is also shown. The very good agreement between the two distributions confirms the proper operation of the WB device, with the latter still allowing for a large room for improvement in the offline analysis.

In conclusion, the tests executed during the 2024 NA64 electron-beam session demonstrated the very good performances of the new "Waveboard" data acquisition board, confirming what was already observed during the first laboratory tests. In preparation for next year's electron-beam run, we plan to replace all MSADC boards for PMT-based detectors with the new devices.

3.2.2 Outcome of LYSO based SRD prototype with positron-beam tests

The extension of the NA64 scientific program to include positron-beam measurements at lower energies, presented for the first time in Ref. [20], necessarily requires upgrading the current Pb/Sc SRD detector. Indeed, through Monte Carlo simula-

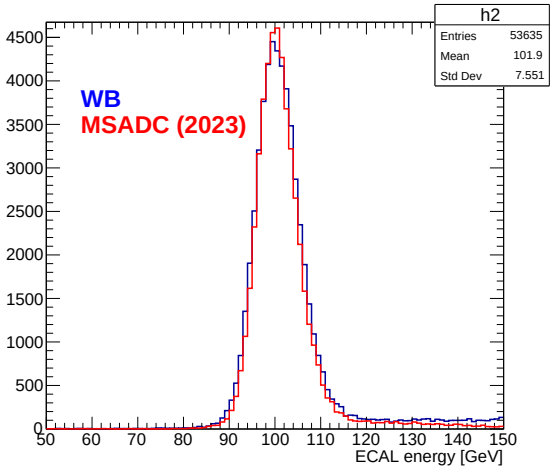

Figure 12. ECAL energy distribution for 100 GeV e^- events, with PMT signals recorded via the new Waveboard device (blue curve), compared with the same observable for a calibration run collected during the 2023 session using the old MSADC devices. For better comparison, the two distributions were normalized to the same value.

tions we observed that, due to the dependency of the synchrotron radiation emission to the fourth power of the impinging $e^{\pm}$ energy, the current detector design would result in a significantly reduced detection efficiency for beam energies lower than $\simeq$70 GeV, even with an optimized Pb-to-Sc ratio. Preliminary studies showed that a fully homogeneous detector made by LYSO crystals, instead, could reach a detection efficiency of up to 85% even at 40 GeV beam energy - the lowest measurement point considered for the program discussed in the aforementioned document.

To validate the studies, we designed a LYSO SRD detector prototype, that was tested during the 2024 70 GeV/c e^+ beam session. The detector is made of six independent modules, each assembled as a matrix of 8×12 LYSO crystals, each $4 \times 4 \times 45$ mm^3 in size. For each module, the scintillation light from crystals is read by a Hamamatsu R7600U PMT, coupled through the crystals via an acrylic light guide. To enhance the light collection, each crystal is individually wrapped in a thin 3M Vikuiti reflection film. Each matrix was hosted in an Aluminum structure to ensure light tightening; to minimize the synchrotron radiation photons absorption, the front face was made as a thin carbon fiber layer - see also Fig. 13, left panel. The six analog PMT signals were connected to a summation card, to allow to acquire each of them with a MSADC channel, and simultaneously use the summed signal in the trigger system. The six modules were installed in the H4 setup, in place of the current Pb/Sc detector, as shown in Fig. 13, right panel. The modules were aligned to have the 3.2×4.5 cm^2 face of each of them exposed to the beam, allowing the synchrotron radiation photons to pass through a total length of 4.8 cm of LYSO active volume.

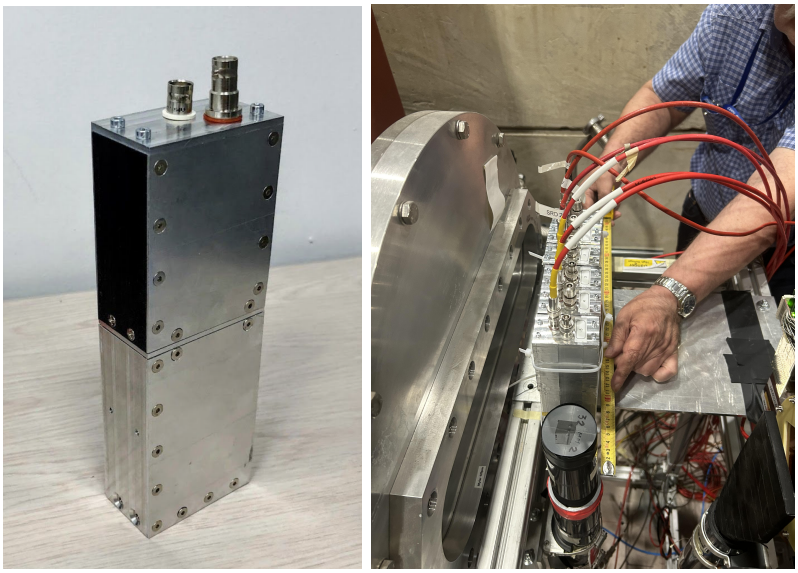

Figure 13. Left: a fully assembled LYSO detector module. Right: the six LYSO modules installed in the NA64 setup during the 2024 test.

The energy response of each module was calibrated with minimum-ionizing particles (MIP). Since, as discussed below, the typical energy deposition of SR photons is significantly lower than that of MIPs, to enhance the detector dynamic range the calibration was performed by rotating each module by 90° to have MIP particles traversing a total length of 3.2 cm in the LYSO (see also Fig. 14). To suppress events with any hadron hard interaction in LYSO crystals, we applied a cut requiring an energy deposition in the MIP range for all six modules, in coincidence with a large energy deposition in the HCAL 3 detector located downstream. The measured energy spectra, in intrinsic ADC units, are reported in Fig. 15, together with the result of a fit performed with a Landau function to extract the most probable value and compare the latter with the prediction from Monte Carlo simulations of about 31 MeV. Incidentally, we observe that the shape of the spectrum for the last LYSO cell is significantly different from the others, possibly because of splash-back effects from HCAL3.

The measured synchrotron radiation total energy distribution for impinging 70 GeV/c e^+ is shown in Fig. 16, together with the prediction from Monte Carlo simulations. Overall, a reasonable agreement is observed. We expect to further improve the quality of the data by optimizing the LYSO module's calibration constants, as well as by checking the effect of fine-tuning the magnetic field value in the simulation (so far, the latter was set to a nominal value of 1.295 T). During the tests, we also verified the effect of including the LYSO detector signal in the trigger system, modifying the nominal experiment trigger condition to include a threshold on the corresponding deposited energy, replacing that on the deposited energy in the ECAL pre-shower section. The corresponding efficiency, evaluated online from the measured events

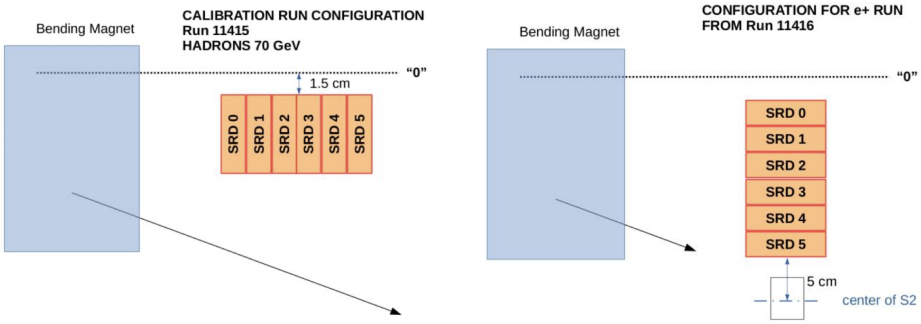

Figure 14. Simplified scheme of the LYSO detector installed in the NA64 detector during the 2024 e^+ test for calibration runs (left) and in the nominal configuration (right).

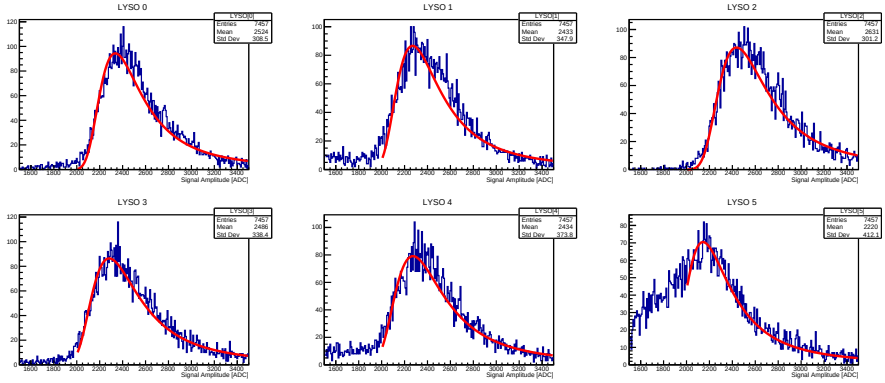

Figure 15. Energy spectra in raw ADC units for each LYSO module, for MIP particles passing through a total length of 3.2 cm. See text for further details.

rate with and without this condition, was larger than 92% for beam intensity up to 7×10^6/spill, for a $\simeq 1.5$ MeV energy threshold.

3.3 Future prospects

The 2016-2024 collected sample corresponds to 2×10^{12} EOT. Our goal before the next long shutdown (LS3) is to collect as much statistics as possible to continue leading the LDM searches in the low mass region and many other leptophilic New Physics searches. In addition, this data will be very important to optimize the detector upgrades planned during LS3. We present two scenarios depending on when LS3 will start:

- At the end of 2025: We plan to request 10 weeks at the beginning of the SPS year, similar to 2022 and 2023 runs. We foresee two weeks for installation and commissioning and 8 weeks for data taking. We will dedicate 7 weeks to the electron and one week to the positron measurements. During this year we plan to equip all the calorimeters with faster digitisers and study the possibility of increasing higher our intensities.

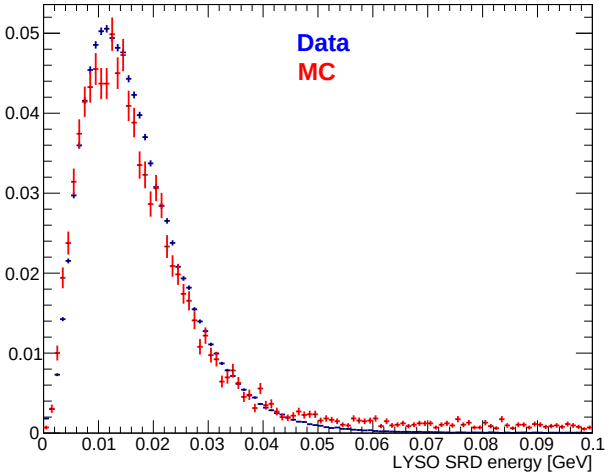

Figure 16. Measured LYSO SRD total energy distribution for impinging 70 GeV/c e^+ (blue), compared with the prediction from MC simulations (red). The two curves have been scaled to the same unitary normalization.

- In 2026: If the shutdown is extended, we would request another 10 weeks depending on beam availability. In this way, we will be able to achieve 3×10^{12} EOT.

4 Summary

The current NA64 run in 2024 has been both successful and productive. All sub-detectors are operating well, allowing us to accumulate high-quality data efficiently. Both the NA64e and NA64μ experiments are expected to yield significant physics results from the combined 2021-2024 data set. The 2025 run will allow us to continue this program to achieve our goals for both physics programs and initiate a new hadron program for the future. With a modest investment of time and budget, NA64 will maintain its position as a world-leading experiment, producing results that cannot be achieved anywhere else in the world on this timescale.
In short, NA64 addresses the following areas in dark sector physics with unprecedented sensitivity:

(i) probe decisively the benchmark LDM parameter space for the scalar and Majorana type of dark matter for the benchmark coupling value $\alpha_D \leq 0.1$

(ii) search for other dark sector physics, such as (pseudo)scalar, vector, axial-vector mediators, $B-L$ Z' and ALP particles, lepton-flavour changing reactions, etc...

(iii) either to confirm or exclude the $L_\mu - L_\tau$ Z' explanation of the muon g-2 anomaly.

5 Publications

The collaboration has published the following results since the last report submitted in September 2023:

(i) Y. M. Andreev, *et al.* [NA64], "50 GeV π^- in, nothing out: a sensitive probe of invisible η and η' decays with NA64h," [arXiv:2406.01990 [hep-ex]].

(ii) Y. M. Andreev *et al.* [NA64], "First constraints on the $L_\mu - L_\tau$ explanation of the muon g-2 anomaly from NA64-e at CERN," JHEP **07** (2024), 212 doi:10.1007/JHEP07(2024)212 [arXiv:2404.06982 [hep-ex]].

(iii) Y. M. Andreev *et al.* [NA64], "First Results in the Search for Dark Sectors at NA64 with the CERN SPS High Energy Muon Beam," Phys. Rev. Lett. **132** (2024) no.21, 211803 doi:10.1103/PhysRevLett.132.211803 [arXiv:2401.01708 [hep-ex]].

(iv) Y. M. Andreev *et al.* [NA64], "Probing light dark matter with positron beams at NA64," Phys. Rev. D **109** (2024) no.3, L031103 doi:10.1103/PhysRevD.109.L031103 [arXiv:2308.15612 [hep-ex]].

(v) Y. M. Andreev *et al.* [NA64], "Search for Light Dark Matter with NA64 at CERN," Phys. Rev. Lett. **131** (2023) no.16, 161801 doi:10.1103/PhysRevLett.131.161801 [arXiv:2307.02404 [hep-ex]].

In addition, NA64 members and, in particular, the theory working group of the Collaboration, have contributed with the following publications related to NA64e and NA64$_\mu$:

1. S. N. Gninenko, D. V. Kirpichnikov, N. V. Krasnikov, S. Kuleshov, V. E. Lyubovitskij and A. S. Zhevlakov, "Probing leptophobic dark sector with a pseudoscalar portal in the NA64 experiment at CERN," [arXiv:2407.01181 [hep-ph]].

2. B. B. Oberhauser *et al.*, "Development of the fully Geant4 compatible package for the simulation of Dark Matter in fixed target experiments," Comput. Phys. Commun. **300** (2024), 109199 doi:10.1016/j.cpc.2024.109199 [arXiv:2401.12573 [hep-ph]].

3. S. N. Gninenko, D. V. Kirpichnikov, S. Kuleshov, V. E. Lyubovitskij and A. S. Zhevlakov, "Test of the vector portal with dark fermions in the charge-exchange reactions in the NA64 experiment at CERN SPS," Phys. Rev. D **109** (2024) no.7, 075021 doi:10.1103/PhysRevD.109.075021 [arXiv:2312.01703 [hep-ph]].

4. A. S. Zhevlakov, D. V. Kirpichnikov, S. N. Gninenko, S. Kuleshov and V. E. Lyubovitskij, "Probing invisible vector meson decay mode with the hadronic beam in the NA64 experiment at SPS CERN," Phys. Rev. D **108** (2023) no.11, 115005 doi:10.1103/PhysRevD.108.115005 [arXiv:2309.09347 [hep-ph]].

5. A. S. Zhevlakov, D. V. Kirpichnikov and V. E. Lyubovitskij, "Lepton flavor violating dark photon," Phys. Rev. D **109** (2024) no.1, 015015 doi:10.1103/PhysRevD.109.015015 [arXiv:2307.10771 [hep-ph]].

6. N. V. Krasnikov, "Dark matter models with suppressed dark matter nuclei elastic cross section," Phys. Lett. B **854** (2024), 138747 doi:10.1016/j.physletb.2024.138747 [arXiv:2405.03325 [hep-ph]].

7. N. V. Krasnikov, "Search for Light Dark Matter at the Accelerators. NA64 Experiment," Phys. Part. Nucl. **54** (2023) no.5, 902-907 doi:10.1134/S1063779623050143

8. I. V. Voronchikhin and D. V. Kirpichnikov, "Probing scalar, Dirac, Majorana, and vector dark matter through a spin-0 electron-specific mediator at electron fixed-target experiments," Phys. Rev. D **109** (2024) no.7, 075012 doi:10.1103/PhysRevD.109.075012 [arXiv:2312.15697 [hep-ph]].

The collaboration has also contributed to several International Conferences and topical Workshops such as ICHEP2024, LLP2024, PBC2024, LDW2023, etc where the latest NA64 physics results and the future prospects were presented.

References

[1] Y. M. Andreev et al. *Nucl. Instrum. Meth. A* 1057, 168776 (2023). doi:10.1016/j.nima.2023.168776.

[2] Y. M. Andreev et al. *Phys. Rev. Lett.* 132, 211803 (2024). doi:10.1103/PhysRevLett.132.211803.

[3] Y. Kahn, et al. *JHEP* 09, 153 (2018). doi:10.1007/JHEP09(2018)153.

[4] M. Solt. *Phys. Sci. Forum* 8, 17 (2023). doi:10.3390/psf2023008017.

[5] R. Godang. *EPJ Web Conf.* 141, 02005 (2017). doi:10.1051/epjconf/201714102005.

[6] R. Capdevilla, et al. *JHEP* 04, 129 (2022). doi:10.1007/JHEP04(2022)129.

[7] A. Kamada and H.-B. Yu. *Phys. Rev. D* 92, 113004 (2015). doi:10.1103/PhysRevD.92.113004.

[8] Y. Kaneta and T. Shimomura. *PTEP* 2017, 053B04 (2017). doi:10.1093/ptep/ptx050.

[9] S. Gninenko and D. Gorbunov. *Phys. Lett. B* 823, 136739 (2021). doi:10.1016/j.physletb.2021.136739.

[10] W. Altmannshofer, et al. *Phys. Rev. Lett.* 113, 091801 (2014). doi:10.1103/PhysRevLett.113.091801.

[11] S. R. Mishra et al. *Phys. Rev. Lett.* 66, 3117 (1991). doi:10.1103/PhysRevLett.66.3117.

[12] A. Berlin, et al. *Phys. Rev. D* 99, 075001 (2019). doi:10.1103/PhysRevD.99.075001.

[13] C.-Y. Chen, J. Kozaczuk, and Y.-M. Zhong. *JHEP* 10, 154 (2018). doi:10.1007/JHEP10(2018)154.

[14] D. Banerjee, P. Crivelli, and A. Rubbia. *Adv. High Energy Phys.* 2015, 105730 (2015). doi:10.1155/2015/105730.

[15] E. Depero et al. *Nucl. Instrum. Meth. A* 866, 196 (2017). doi:10.1016/j.nima.2017.05.028.

[16] Y. M. Andreev et al. *Phys. Rev. Lett.* 131, 161801 (2023). doi:10.1103/PhysRevLett.131.161801.

[17] S. N. Gninenko and N. V. Krasnikov. *Phys. Rev. D* 106, 015003 (2022). doi:10.1103/PhysRevD.106.015003.

[18] A. Ponten, et al. (2024).

[19] L. R. Dalesio, et al. *Nucl. Instrum. Meth. A* 352, 179 (1994). doi:10.1016/0168-9002(94)91493-1.

[20] P. Bisio, et al. Light dark matter search with positron beams at NA64. Technical report, CERN, Geneva (2024).